Wetting of Oriented and Etched Ultrahigh Molecular Weight Polyethylene

M. S. SILVERSTEIN, J. SADOVSKY, D. ALON, V. WAHAD

Department of Materials Engineering, Technion-Israel Institute of Technology, Haifa 32000, Israel

Received 20 July 1998; accepted 20 August 1998

ABSTRACT: Highly oriented gel-spun ultrahigh molecular weight polyethylene (UHMWPE) fibers possess many outstanding properties desirable for composite materials but their adhesion to such matrices as epoxy is poor. This article describes the combined effects of drawing and surface modification on the bulk and surface properties of gel-cast UHMWPE films emphasizing the effects of etching on both undrawn and drawn films. Drawing the films yields a fibrillar structural hierarchy similar to UHMWPE fibers and a significant increase in orientation, melting point, modulus, and strength. The effects of drawing on bulk properties were more significant than those of etching. The poor adhesion of epoxy to the smooth, fibrillar, and relatively nonpolar drawn film surface improves significantly with oxidization and roughening on etching. The interlaminar shear failure occurred cohesively in the UHMWPE, and thus the interlaminar shear failure strength was greater for the drawn UHMWPE with its greater tensile strength. Nitrogen plasma etching yielded the best results, both removing any low molecular weight surface layer and etching the UHMWPE beneath. Oxygen plasma etching enhanced wetting but was too harsh, causing extensive surface degradation and a significant reduction in mechanical properties. © 1999 John Wiley & Sons, Inc. J Appl Polym Sci 72: 405–418, 1999

Key words: ultrahigh molecular weight polyethylene; wetting; orientation; plasma etching; chromic acid etching

INTRODUCTION

Gel-spun ultrahigh molecular weight polyethylene (UHMWPE) fibers are highly oriented and thus possess many outstanding properties that are desirable in fibers for composite materials.[1] These desirable properties include superior toughness, chemical resistance, and biocompatibility. The melting point, modulus, and strength increase with increasing crystalline orientation.[1,2] Unfortunately, the inclusion of UHMWPE fibers in composite materials has been limited by their poor adhesion to polymer matrices.[3]

Gel processing can leave a weak boundary layer on the surface of UHMWPE fibers from the oxidized residue of solvents, processing aids, and low molecular weight polymer.[4,5] Surface modification is used to remove weak boundary layers, roughen the surface to enhance mechanical interlocking, and form chemical groups on the surface that enhance wetting and/or chemical bonding. Chromic acid (CA) attacks polyethylene through hydrogen abstraction, preferentially in the amorphous region.[4,5] The etched surface is roughened significantly and includes oxidized groups yielding enhanced wetting by epoxy and the formation of a stronger bond with epoxy.[4,6,7] Previous work investigating the effects of various chemical etchants on gel-spun UHMWPE fibers found that CA etching yields a particularly large improve-

Correspondence to: M. S. Silverstein.

Journal of Applied Polymer Science, Vol. 72, 405–418 (1999)
 CCC 0021-8995/99/030405-14

ment in wetting and adhesion to epoxy.[8–12] Unfortunately, the fibers became embrittled on prolonged etching and the improvement in wetting and adhesion was accompanied by reduced mechanical properties. Plasma etching has similar effects on wetting, adhesion, and mechanical properties.[13–19]

Casting a very dilute UHMWPE gel with minimal entanglements yields a film that can be oriented by drawing at temperatures somewhat below the melting point.[20–25] The resulting films have a fibrillar structural hierarchy similar to that seen for the UHMWPE fibers.[9,26] Planar uniaxially oriented gel-cast UHMWPE films were used as a model system for the study of gel-spun UHMWPE fibers and behaved in a similar fashion.[26]

This article describes two aspects of the continuing investigation of these UHMWPE fibers and films. The first is the combined effects of drawing and surface modification on the bulk and surface properties of gel-cast UHMWPE films emphasizing the different effects of etching on undrawn and drawn films. The second is the relationship between plasma etching conditions and wetting.

MATERIALS AND METHODS

Materials

The films were made by gel-casting a solution of 0.5 wt % 3×10^6 g/mol molecular weight UHMWPE powder (Hostalen GUR 402, Hoechst, Germany) in decalin (decahydronaphthalene, Spectrum, Gardena, CA). The UHMWPE powder contained 0.5% (w/w) antioxidant (Plastanox 2246, Cyanamide, Stamford, CT). The transparent solution formed after stirring at 160°C for 45 min was cast into a glass dish, left in an oven at 65°C for 24 h, immersed in ethanol for 2 h to extract decalin, rinsed with distilled water, and then dried in a vacuum oven at 25°C for 24 h. These films, approximately 90 μm thick, will be referred to as the *as-cast* films. The as-cast films were oriented uniaxially to draw ratios (DR) up to 60 at 120°C by hanging a 200-g weight from the bottom of a vertical 1.7-cm-wide strip and allowing the strip to reach a predetermined extension. Commercial gel-spun UHMWPE fibers were used in this investigation [Spectra 1000, 650 denier (g/9000 m), Allied Signal, Petersburg, VA)]. The epoxy (DER324, Dow Chemical, Midland, MI) was used without a curing agent for contact angle measurements and with a curing agent for the interlaminar shear strength (ILSS) measurements. The curing agent (ethylenediamine, Fluka, Switzerland) was added to the epoxy in a mass ratio of 1 : 10.

Surface Modification

The chemical etching procedure found to yield the maximum increase in wetting and adhesion to epoxy was used.[8,11] The chemical etching was carried out in CA at 25°C for 4 h and the etched films then were washed with distilled water and is referred to as CA1.

A commercial plasma etcher (Jupiter III, March Instruments, Concord, CA) was used for plasma etching.[26] The UHMWPE film was placed on the lower electrode, which was cooled to 20°C using a recirculating coolant (RTE-110, Neslab, Newington, NH). After etching, the plasma reactor was evacuated to 2.5 Pa, purged with argon, and opened to the atmosphere. In the initial stages of this investigation one set of oxygen plasma etching conditions was used for the UHMWPE films (10 min at a power of 50 W and a pressure of 67 Pa) and is referred to as OP1.

Following the initial investigation, the plasma etching conditions were changed to study the relationships between plasma conditions and wetting. The films and fibers were etched at 133 Pa in oxygen, argon, or nitrogen at various powers (2–300 W) and for various times (10 s–5 min). One series of experiments evaluated the effect of postetching oxygen exposure by introducing oxygen at 133 Pa for various times (30 s–5 min) prior to opening the reactor to the atmosphere.

Bulk Characterization

The melting points and degrees of crystallinity were characterized through differential scanning calorimetry (DSC) (Mettler TC10A, Switzerland). The film was heated from room temperature to 160°C at 10°C/min and the crystallinity was calculated assuming a heat of fusion of 280 J/g.[27] The crystalline orientation in the films was characterized through wide angle X-ray scattering (WAXS) (PW1840, Philips, Netherlands) using a CoK_α source (0.179 nm wavelength) without a monochromator. Transmission Fourier transform infrared spectroscopy (FTIR) (IFS48, Bruker, Germany) was used to investigate the molecular structure of the bulk.

The modulus and strength were determined in uniaxial tension using a tensile tester (JJ T5002,

Lloyd Instruments, UK). Strips of film 1.5 cm in length were strained at 5 cm/min (333%/min). Strips of the CA etched films 1.0 cm long were tested at the same crosshead speed and thus at a higher strain rate (500%/min). The tensile modulus was taken from the steepest slope in the initial part of the stress–strain curve and the tensile strength from the maximum force attained.

Surface Characterization

The topographies of the films and fibers were determined using both scanning electron microscopy (SEM) and atomic force microscopy (AFM). The SEM (JEOL JSM-840, Japan) specimens were coated with a 0.02-μm layer of evaporated gold. The AFM (Topometrix TMX 2010 Discoverer, Santa Clara, CA) was used in noncontact mode. Electron spectroscopy for chemical analysis (ESCA) was used to characterize the surface chemistry using an AlK_α source and a 40° angle of incidence (Physical Electronics 555 ESCA/Auger, Perkin Elmer, Eden Prairie, MN). The overall spectrum was taken at low resolution and the spectra of elements of interest were taken at high resolution. The high-resolution spectra were deconvoluted to describe more accurately the contributions of different bonds to the overall peak.[26]

Wetting

Films

The wetting of the UHMWPE films was described through the advancing contact angle technique[5] with an accuracy of 1° using a Kernco goniometer. The droplets on the undrawn films were circular, as expected. However, the epoxy droplets on the drawn films were ellipsoidal. The major axis of the ellipse was in the draw direction and the contact angle was measured in that direction unless otherwise stated. Epoxy was used for the contact angle measurements in the initial stages of the investigation and later distilled water was used.

Fibers

The wetting of the UHMWPE fibers was characterized using the fiber flotation technique illustrated schematically in Figure 1 that was described in detail previously.[11] The apparatus consists of a beaker containing a liquid covered by a watch glass. The watch glass has a center slot from which 1-cm-long fiber sections can be rolled gently into the beaker. The fiber flotation for a given liquid is the percentage of fiber sections that float on the surface from a sample of >100.

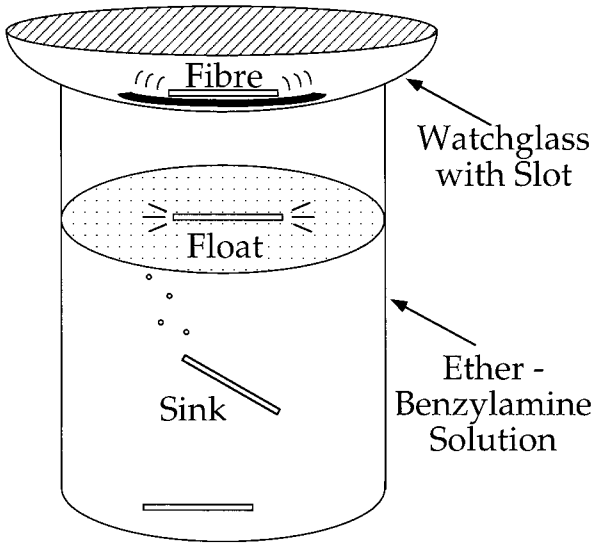

Figure 1 Schematic diagram of fiber flotation.

The following are the two extreme situations: the fiber sections are not wet completely by a very high surface tension liquid and 100% float; the fiber sections are wet completely by a very low surface tension liquid and 100% sink. A step-function transition is expected at a surface tension between these two extremes. Practically, the measured transition is somewhat smoother and the float–sink transition is defined as the liquid surface tension where 50% of the fiber sections sink. The force balance on a floating fiber shows that at the float–sink transition the fiber surface energy is proportional to the liquid surface tension.[11]

Solutions of diethyl ether (ether, Fluka, Switzerland) and benzylamine (Fluka, Switzerland) are the liquids used here, a great improvement on those used in previous experiments. The surface tensions of ether and benzylamine, 16.7 and 39.3 mN/m,[28] respectively, provide the low surface tension and high surface tension extremes. The solutions are expected to have surface tensions roughly symmetric to a straight line connecting the surface tensions of the pure liquids.[29] Flotation curves show the variation of the fiber flotation with ether concentration and the float–sink transition is taken as the composition at which 50% of the fiber sections sink.

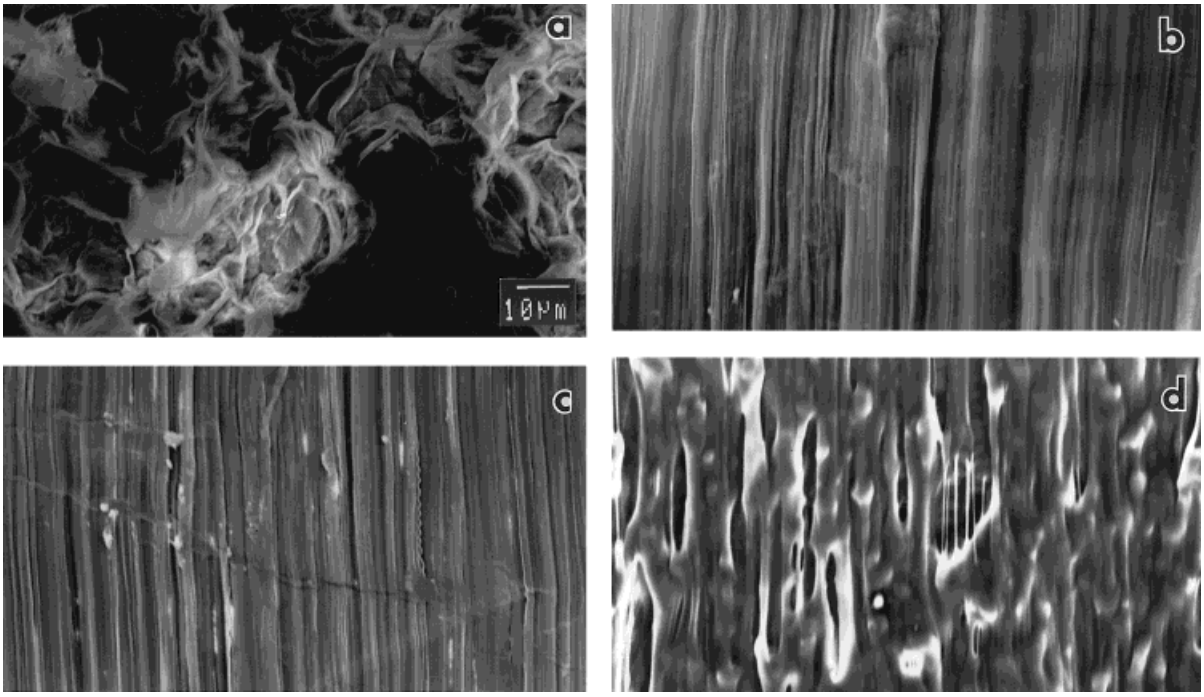

Figure 2 SEM micrographs of UHMWPE films; DR = (a) 1, (b) 10, (c) 20, and (d) 60.

Adhesion

The adhesion of epoxy to the UHMWPE films was characterized using the Al/epoxy/UHMWPE/epoxy/Al (five-layer sandwich) ILSS specimens described previously.[26] Basically, a 2 × 0.2 cm aluminum strip was bonded to each side of a 1 × 0.2 cm UHMWPE film with epoxy such that a 1-cm aluminum tab extended from each end of the five-layer sandwich. The epoxy was cured by placing the ILSS specimen in an oven at 80°C for 5 h under a 200-g weight. The specimen was removed from the oven and tested in shear at room temperature using a tensile tester (JJ T 5002, Lloyd Instruments) by placing the aluminum tabs in the grips. The failure surfaces were coated with a 0.02-μm layer of evaporated gold and examined in the SEM.

RESULTS AND DISCUSSION

Fibrillar Structure in UHMWPE Films

The film surfaces are seen in Figures 2, 3, and 4. The fibrils on the rough surface of the as-cast film [Fig. 2(a)] extend three-dimensionally. The arrangement of fibrils on the surface can be affected by the casting, extraction, and drying processes. A DR of 10 yields a relatively smooth surface with a highly oriented fibrillar structure in the draw direction [Fig. 2(b)]. Fibrils of approximately 1 μm are gathered into interconnected and partially merged bundles of approximately 10 μm. At a DR of 20 [Fig. 2(c)] the bundles are approximately 5 μm and they are more distinctly separate from neighboring bundles.

The large gaps between the bundles at a DR of 60 [Fig. 2(d)] are elongated in the orientation direction. Necking and failure occur within individual bundles at high DRs. The stress on a bundle relaxes following failure at the high drawing temperature producing the round knobs in Figure 2(d). The ends of the broken bundles are drawn apart as drawing continues leaving an elongated hole.

The hierarchical nature of the fibrillar structure of a UHMWPE film with a DR of 50 is confirmed in the AFM micrographs in Figure 3. Parallel fibrils approximately 200 nm in diameter within 5-μm bundles are seen at lower magnification [Fig. 3(a)]. A similar but significantly smaller fibrillar structure, with fibrils approximately 10 nm in diameter, is seen at higher magnification [Fig. 3(b)].

Etching yields drastic changes in the topography of the undrawn film. The fibrils extending

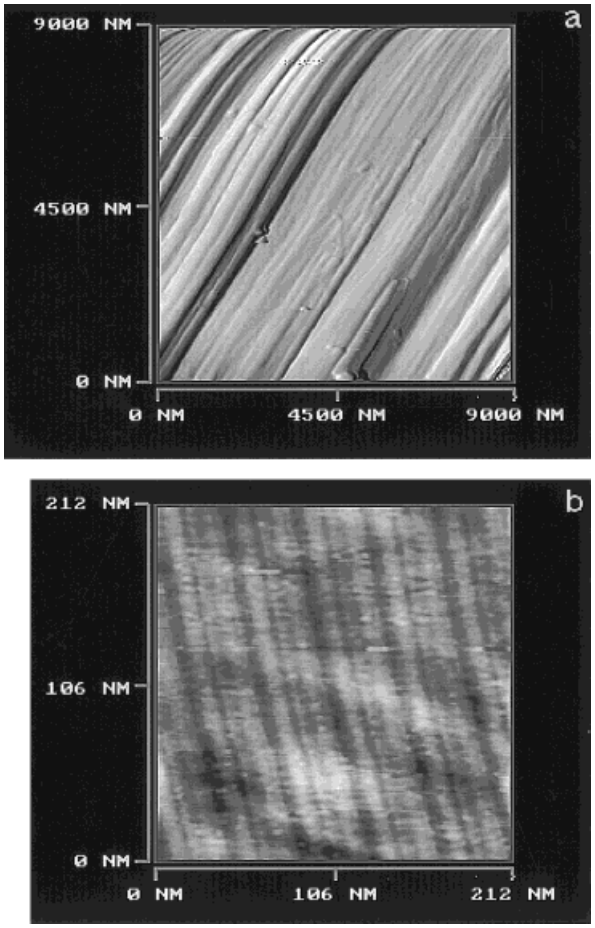

Figure 3 AFM micrographs of UHMWPE film; DR = 50: (a) low resolution and (b) high resolution.

from the film surface are removed by both CA and oxygen plasma etching [Fig. 4(a) and (b), respectively]. Etching removed the fibrils on the surface leaving a rough pitted surface. In contrast, the oriented fibrillar topography of the drawn films seems barely affected by CA or oxygen plasma etching [Fig. 4(c) and (d), respectively]. Although the plasma-etched drawn film is roughened slightly, the changes in topography [Figs. 1(c) and 4(d)] are minor compared with those in the undrawn film [Figs. 1(a) and 4(b)]. The fibrillar structure of the plasma-etched drawn film does not seem as distinct and there is some merging of the fibril bundles. The merging of fibrils may result from film heating during plasma exposure.

Crystalline Structure

The as-cast UHMWPE film has a melting point (T_m) of 136°C and exhibits a single endothermic DSC peak. The drawn films exhibit a wide endothermic DSC peak with two maxima: a lower melting point at 136°C and an upper melting point at a temperature several degrees higher. Both the position (Fig. 5) and the relative height of the upper melting peak increases with DR. The position of the lower melting peak is unaffected by drawing, but its relative height decreases with DR. The two melting points indicate that there are two types of crystals, the original crystals formed on casting and those formed during drawing. The increase in the relative height of the upper melting peak and in the upper melting point on drawing is associated with increasing amounts of the oriented crystalline structure and increasing crystalline perfection.[30–32] The upper melting point reaches an asymptote at high DRs (Fig. 5) near the theoretical T_m.[27]

There is relatively little change in the melting peak on etching with CA. The reversion of the crystals formed during drawing to a less ordered and less perfect structure on oxygen plasma etching is reflected in the larger decrease in melting point for the drawn films in Figure 5. The decrease in melting point on etching is indicative of the changes in bulk properties that are undesirable by-products of this harsh etching process. Chemical degradation during etching[9] can be more significant here because a much larger fraction of the thin film bulk is affected than is affected in thicker molded sections. The significant effects of surface modification on the bulk properties of 30-μm-diameter UHMWPE fibers also have been ascribed to the relatively large fraction of the cross section affected by etching.[8,12] Heating of the film due to insufficient cooling during high-energy plasma bombardment also may contribute to changes in the bulk properties on plasma etching. The proportion of the bulk affected by heating increases with decreasing thickness and is more significant for the drawn films, which are thinner than the undrawn films.

The degree of crystallinity from the area of the endothermic DSC peak is seen in Figure 6. The slight reduction in degree of crystallinity on reaching a DR of 10 can be ascribed to the breakup of the original unoriented crystals prior to their orientation as well as the differences in thermal history after drawing at 140°C.[33,34] The crystallinity increases on drawing further as more oriented, extended crystalline blocks are formed. The decrease in crystallinity for DR = 60 can be associated with fibril failure and relaxation, as seen in Figure 2(d). The effects of CA etching on the degree of crystallinity is relatively

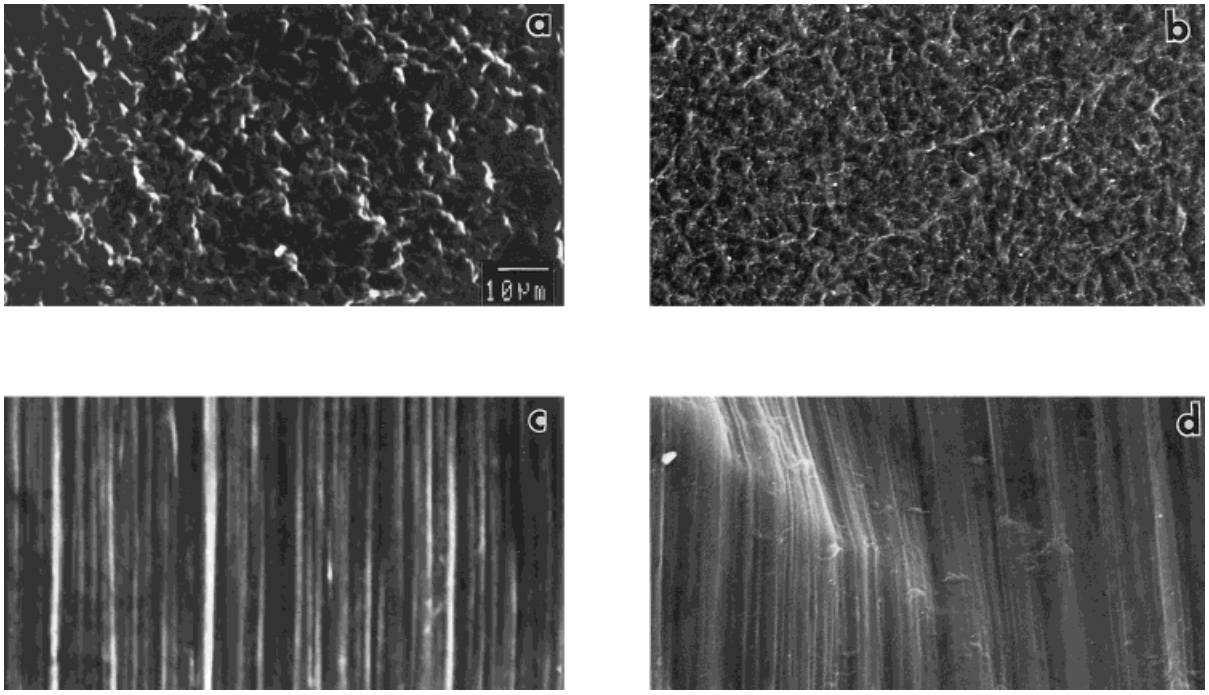

Figure 4 SEM micrographs of etched UHMWPE films: (a) and (b) undrawn; (c) and (d) DR = 20; (a) and (c) CA1; (b) and (d) OP1.

small. The effects of oxygen plasma etching on the degree of crystallinity is more significant, especially for the drawn films. Here again, the thinner drawn films are more sensitive to the effects of etching than the undrawn films.

The effects of drawing on crystal structure are far more significant than those of surface modification, as seen in the WAXS spectra in Figure 7. The undrawn films were thicker and would therefore have been expected to yield higher intensity peaks. In fact, the peak intensities for the undrawn films were a factor of 10 smaller than those for the drawn films. The intensities of the undrawn films have been multiplied by 10 for display in Figure 7 whereas the intensities of the drawn films are unmodified. The spectra from the undrawn films exhibit peaks of similar magnitude representing d-spacing of 4.1, 3.7, 2.25, 2.2, 2.1, and 2.0 Å. These peaks correspond to the (110),

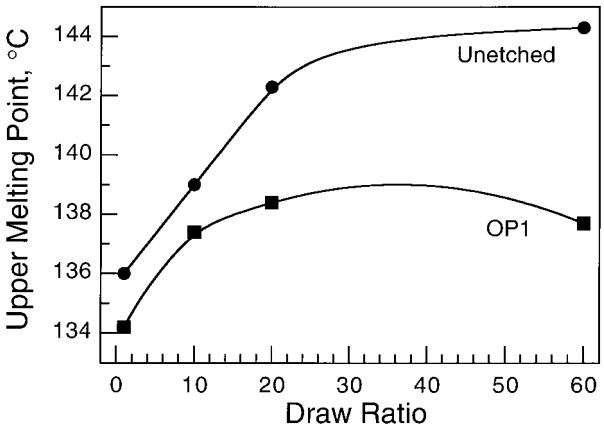

Figure 5 Upper melting points of UHMWPE films: (●) unetched and (■) OP1.

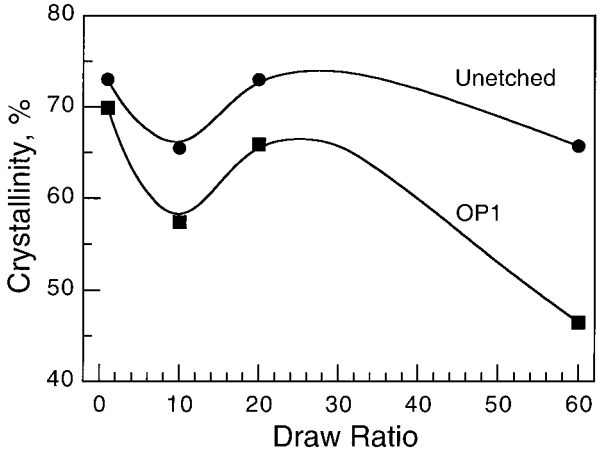

Figure 6 Degrees of crystallinity of UHMWPE films: (●) unetched and (■) OP1.

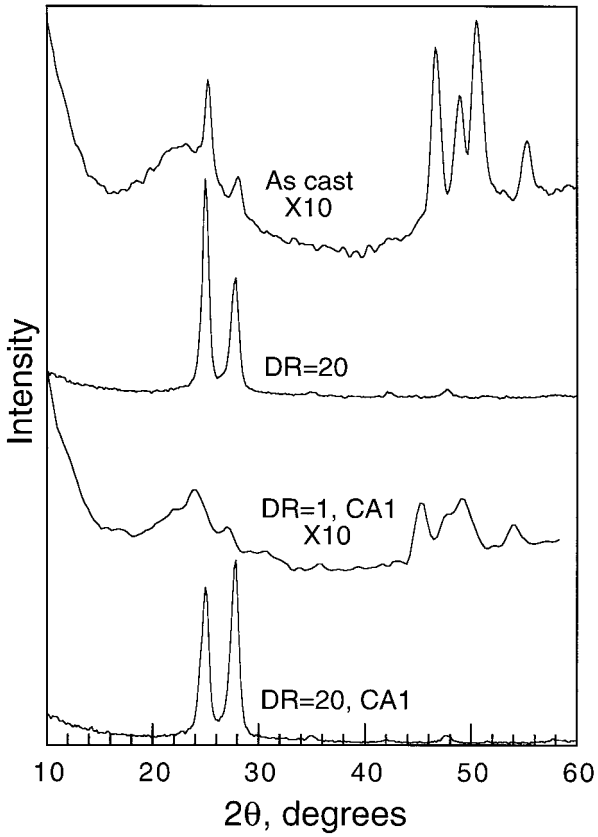

Figure 7 WAXS spectra of UHMWPE films.

(200), (120), (310), (201), and (400) plane spacings of an orthorhombic polyethylene crystal[1] with a, b, and c axes of 0.74, 0.49, and 0.25 nm, respectively. The wide amorphous peak is obvious in the spectra of the undrawn films. The spectra of the drawn films are quite different. There are only two prominent peaks, representing d-spacings of 4.1 and 3.7 Å, whose intensities are 10-fold those in the undrawn films. The crystals are oriented such that the c axis, the direction of the polymer chains, lies in the plane of the film and does not produce scattering peaks.

The WAXS spectra for the etched undrawn and drawn films also are found in Figure 7. The CA etching does not affect the 10-fold difference in intensity between the drawn and undrawn films and has a small effect on the relative heights of the peaks compared with the spectra of the unetched films. Overall, the changes in the WAXS spectra on CA etching are minor compared with the significant changes effected by drawing.

Molecular Structure—Bulk

The transmission FTIR spectra in Figure 8 reflect the molecular structure of the bulk. The as-cast film FTIR spectrum has both the relatively major peaks (2850–3000 cm^{-1}, 1450–1470 cm^{-1}, and 720–725 cm^{-1}) and the relatively minor peaks (1360, 1900, 2640, and 3600 cm^{-1}) typical of UHMWPE.[35] Drawing decreases the prominence of the minor peaks indicating changes in crystalline orientation, perfection, and structure.[36] Etching increases the prominence of the minor peaks indicating a reduction in crystalline orientation and perfection.

Mechanical Properties

The tensile modulus and tensile strength (Fig. 9) increase by over an order of magnitude when the film is drawn to a DR of 10, as expected.[1,31,34] Further orientation yields increases in mechanical properties reaching asymptotes at DR = 60 reflecting the limitations of this particular drawing process. Further increases in mechanical properties could be produced by optimizing the drawing conditions or by using a two-stage draw-

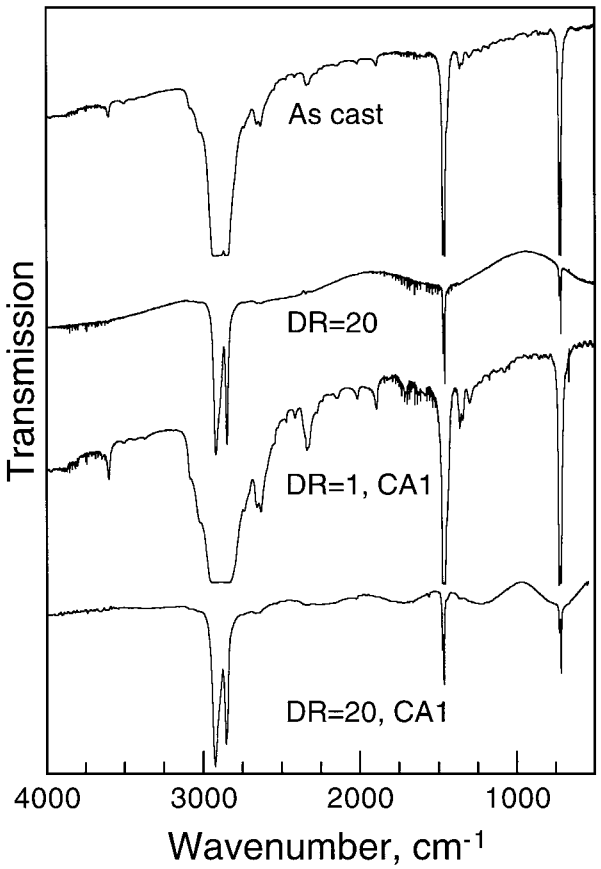

Figure 8 Transmission FTIR spectra of UHMWPE films.

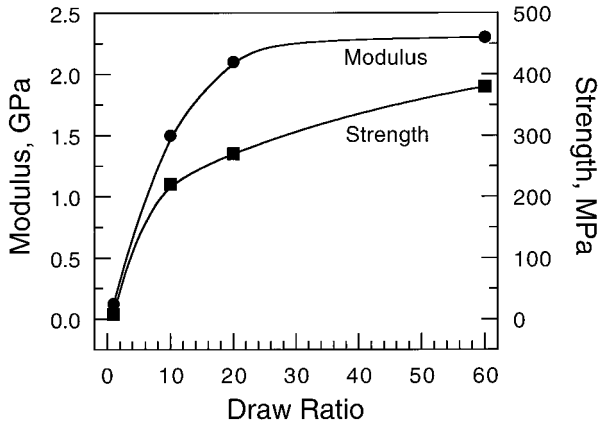

Figure 9 Mechanical properties of unetched UHMWPE films: (●) modulus and (■) strength.

ing process.[33,34,37] The significant increase in mechanical properties on drawing is related directly to the significant increase in crystalline orientation seen in the WAXS spectra and not to the rather insignificant variations in the degree of crystallinity. The mechanical properties of the CA etched films are approximately 67–80% of the unetched films (Table I) in spite of being tested at a higher strain rate. Overall, drawing yields a far more significant effect on modulus and strength than etching, in keeping with its effects on orientation.

Molecular Structure—Surface

The ESCA indicates that the surface of the as-cast film contains 8.0 at. % oxygen. The deconvolution of the C_{1s} spectrum yielded peaks at 285 eV (carbon—carbon), 286.5 eV (hydroxyl, ether, and aldehyde), 288 eV (carbonyl), and 289.5 eV (carboxyl). The ratios of the different peak areas (A_{peak}) to the total C_{1s} peak area (A_T) are listed in Table II. The deconvolution shows that the majority of the 8 at. % oxygen in the as-cast film is attributed to single carbon—oxygen bonds.

Table I Mechanical Properties of UHMWPE Films

		Modulus (GPa)	Strength (MPa)
DR = 1	Unetched	0.12	7.4
	CA1	0.10	5.2
DR = 20	Unetched	2.1	270
	CA1	1.4	200

Table II Atomic Compositions of UHMWPE Film Surfaces

	Unetched		CA1	
	DR = 1	DR = 20	DR = 1	DR = 20
0, at. %	8.0	3.1	13.6	20.7
Si, at. %	—	—	—	8.5
$A_{286.5}/A_T$	3.0	1.7	4.2	0.0
A_{288}/A_T	0.0	1.3	3.4	3.9
$A_{289.5}/A_T$	0.0	1.2	0.0	2.4

Drawing the film reduces the amount of surface oxygen to 3.1 at. % with similar amounts of all three types of carbon—oxygen bonds. The significant oxygen content on the surface of UHMWPE fibers has been ascribed to the presence of a weak boundary layer formed by oxidized solvent, processing aids, and low molecular weight fragments.[9–12] The oxygen on the surface of the as-cast film may originate in the same manner and drawing at high temperatures would reduce the oxygen content through the evaporation of volatile oxidized moieties.

Etching the undrawn film in CA yields an increase in surface oxygen (Table II) that is associated largely with carbonyl groups and is similar to the changes seen on etching UHMWPE fibers in CA.[10] A slight increase in the carbonyl peak on CA etching also is seen for the film with a DR of 20. There are no significant carbon—oxygen peaks in the C_{1s} spectrum indicating that the majority of the 20.7 at. % oxygen on the etched drawn film (Table II) is bound to the 8.0 at. % silicon contaminating the surface. Etching in an oxygen plasma has a much larger effect yielding 13.6% oxygen on the surface of a film with DR = 20 (with no trace of a silicon contaminant).

Wetting—Chromic Acid and Oxygen Plasma Etching

Although the epoxy droplets on the undrawn films are circular, the droplets on the oriented films are ellipsoidal with the major axis parallel to the direction of fibril orientation.[26] The decrease in the epoxy contact angle from the undrawn to drawn films (Fig. 10) results from this topographically produced change in droplet shape and no conclusions can be drawn regarding wetting. The line connecting the contact angles of the undrawn and drawn films in the figures is used only as an aid to the eye. Drawing yields a

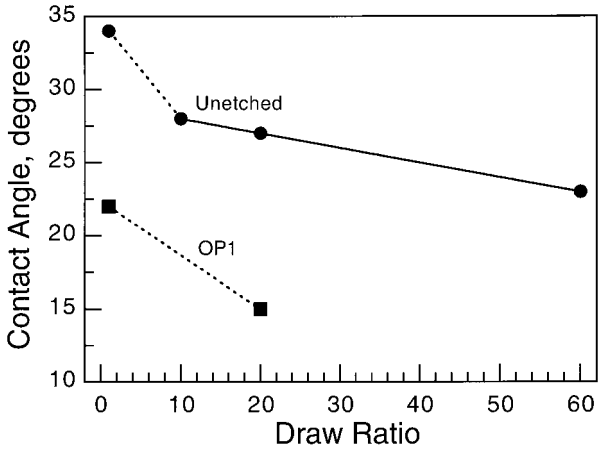

Figure 10 Contact angles of epoxy on UHMWPE films: (●) unetched and (■) OP1.

smoother film with a lower surface oxygen content, both of which are expected to reduce wetting and increase contact angle.[5] The slight reduction in contact angle with drawing from DR = 10 to DR = 60 most likely results from changes in droplet shape and film topography.

The droplet shape is unaffected by etching and so a comparison between unetched and etched films can be made. As expected, the UHMWPE–epoxy contact angles decreased on etching (Fig. 10). The contact angles with the undrawn and drawn films decrease by approximately 12° on both CA and oxygen plasma etching. This enhancement in wetting results from increases in surface oxidation and surface roughness. The roughness of the drawn films is relatively unaffected by etching and the enhancement in wetting results from surface oxidation.

Adhesion

The adhesion of epoxy to the relatively rough and oxygen-rich as-cast film results from a combination of mechanical interlocking and chemical bonding. Drawing, which reduced surface roughness and surface oxidation, also drastically reduced adhesion, as seen in Figure 11. An ILSS specimen could not even be prepared from the drawn but unetched films because there was not even minimal epoxy–UHMWPE bonding. This poor bonding observed for the drawn UHMWPE film is similar to that observed for oriented UHMWPE fibers.[9] Etching the films increases roughness and oxidation, improving wetting and adhesion (Figs. 10 and 11).

The UHMWPE fibrils were pulled out from both sides of the ILSS specimen with the as-cast film. The matching fracture surfaces are seen in Figure 12(a) where area *b*1 from one side of the fracture is enlarged in Figure 12(b) and area *b*2 from the other side of the fracture is enlarged in Figure 12(c). These fracture surfaces show a failure that was largely in the UHMWPE and indicate that the UHMWPE–epoxy bond strength was greater than the UHMWPE cohesive strength.

The adhesion of epoxy to the undrawn films is somewhat improved by both CA and oxygen plasma etching, as seen in Figure 11. The improvement in the adhesion of epoxy to the drawn films is quite pronounced. The interlaminar shear strengths of the etched drawn films are greater than those of the etched undrawn films. Etching improves adhesion through surface oxidation and roughening and the failure is no longer solely at the interface. Failure occurs within the UHMWPE and it is the significantly improved mechanical properties of the drawn UHMWPE that yield the increase in epoxy–UHMWPE bond strength. The failure in the CA etched films tends to be cohesive within the UHMWPE whereas that in the more brittle oxygen plasma etched films tends to be a combination of UHMWPE cohesive failure and failure at the UHMWPE–epoxy interface.[26] This difference in failure mechanisms between CA1 and OP1 holds true for both the undrawn and the drawn films and originates in the relative harshness of oxygen plasma etching.

Wetting—Undrawn Film, Plasma Etching

The contact angle with distilled water immediately following plasma exposure was measured

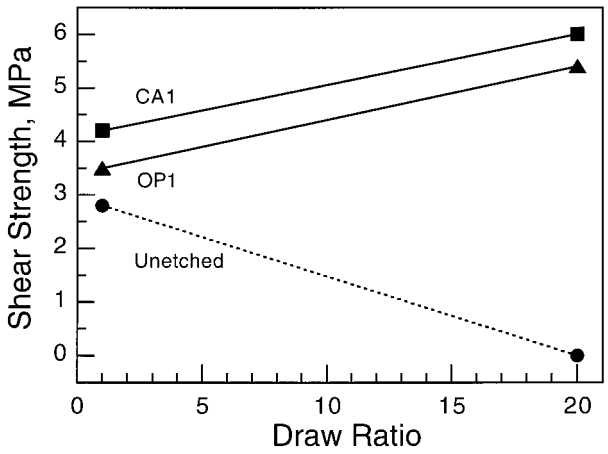

Figure 11 Interlaminar shear strength of five-layer sandwich specimens: (●) unetched, (■) CA1, and (▲) OP1.

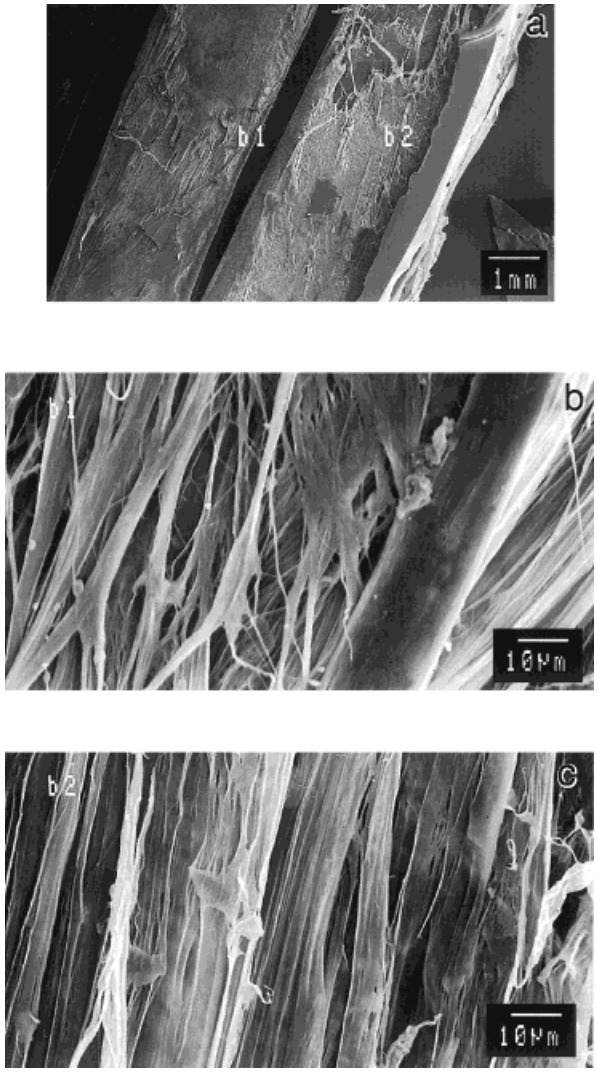

Figure 12 SEM micrographs of ILSS specimen fracture surfaces for as-cast film. (a) Matching surfaces at low magnification showing area *b*1 on one fracture surface and area *b*2 on the matching surface; (b) higher magnification of *b*1; (c) higher magnification of *b*2.

for various gases, plasma powers, etching times, and postetching treatments. The contact angle with the as-cast film was 142°. Etching with any of the gases (oxygen, argon, or nitrogen) at low powers (3.5 W) for even long times (5 min) yielded similar contact angles of approximately 55°, as seen in Figure 13. The gases yield quite different results at higher powers (Fig. 13). The largest decrease in contact angle occurs for a nitrogen plasma at powers greater than 100 W and for oxygen at 300 W (the maximum power available).

The contribution of topography to the contact angles with undrawn films can be seen in the SEM micrographs in Figure 14. The as-cast film [Fig. 14(a)] is somewhat roughened by etching in N_2 at 2 W [Fig. 14(b)] and is roughened significantly by etching in N_2 at 100 W [Fig. 14(c)]. There seems to be an optimal plasma exposure time of approximately 2 min, even at low powers, as seen in Figure 15. As seen previously, the different gases yield similar results after a very short exposure or after a relatively long (5 min) exposure. The results are quite different after a 2-min exposure, with a nitrogen plasma producing the lowest contact angle among the low-power plasmas. The high-power nitrogen plasma consistently produces the lowest contact angles and also exhibits a minimum at 2 min. This minimum may result from reaching an optimum in roughness and surface oxidation. Exposure to oxygen prior to atmospheric exposure after etching in Ar at 5 W yields a significant increase in contact angle in Figure 16. This increase in contact angle with oxygen exposure occurred for all the gases and powers studied.

Wetting—Drawn Film, Plasma Etching

The contact angles measured parallel and perpendicular to fibril orientation for unetched and etched films can be seen in Figure 17. The large contact angle for the unetched film is typical of UHMWPE. The contact angle decreases with DR whether measured parallel or perpendicular to fibril orientation. The initial abrupt decrease in contact angle reflects the change from circular to elliptical droplets. The reduction with further drawing may reflect the extension of the elliptical droplet's major axis with increasing fibrillar ori-

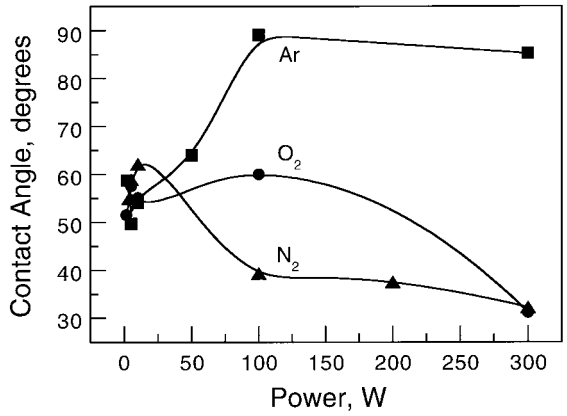

Figure 13 Contact angles of water on undrawn UHMWPE films exposed to different plasmas at various powers: (●) O_2, (■) Ar, and (▲) N_2.

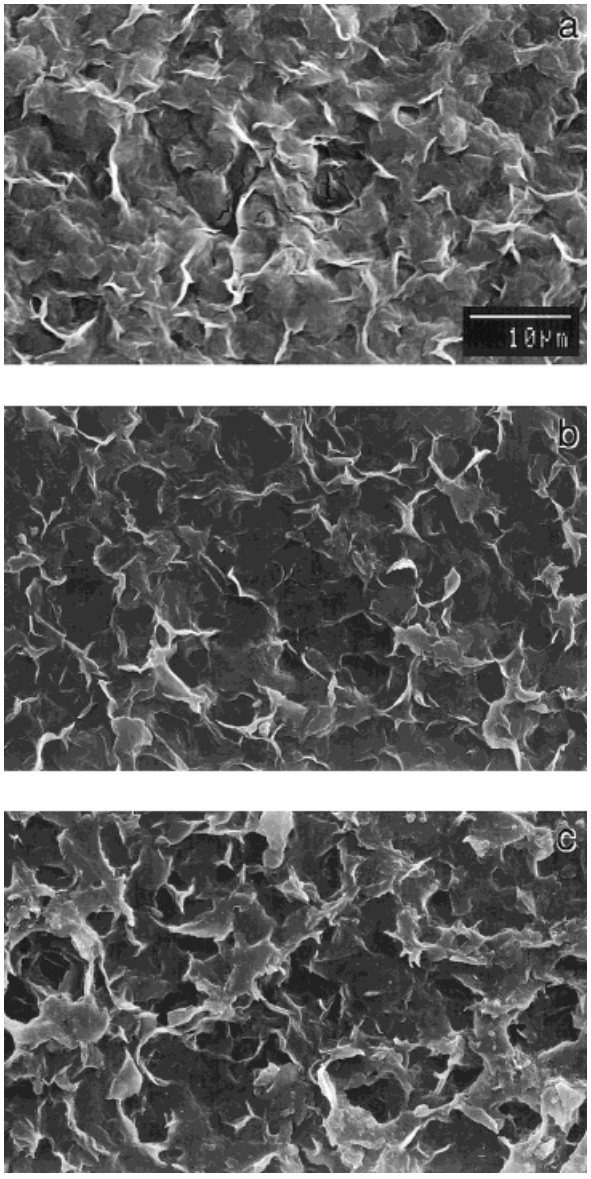

Figure 14 SEM micrographs of undrawn UHMWPE films after 5-min plasma etching: (a) unetched; (b) N_2, 3.5 W; and (c) N_2, 300 W.

entation. Etching reduces the contact angle of both the undrawn and the drawn films in a similar manner. The contact angles from Figure 17 parallel to fibril orientation subtracted from the contact angles perpendicular to fibril orientation yield a difference Δ in Figure 18. The difference between the two perpendicular directions increases with drawing following the changes in topography and reaching a plateau at DR = 20. As the topography is relatively unaffected by etching, so is the difference in contact angles.

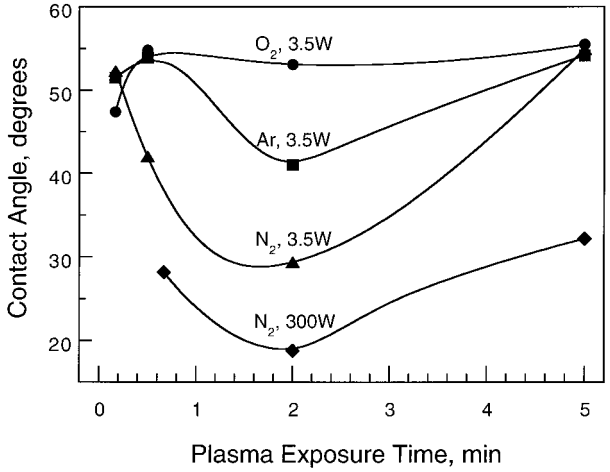

Figure 15 Contact angles of water on undrawn UHMWPE films exposed to different plasmas for various times: (●) O_2, 3.5 W; (■) Ar, 3.5 W; (▲) N_2, 3.5 W; and (◆) N_2, 300 W.

Wetting—Fibers

Fiber flotation curves for plasma-etched fibers on benzylamine-ether solutions are seen in Figure 19. The smooth float–sink transitions are a great improvement on the more complex curves produced using water-propylamine solutions.[11] The float–sink transition for all the etched fibers occurs at a lower ether concentration, in a higher surface tension liquid, than for the as-received fibers. This change in the transition indicates that etched fibers are completely wet by a higher surface tension liquid whereas the unetched fibers are not. This enhancement in wetting is

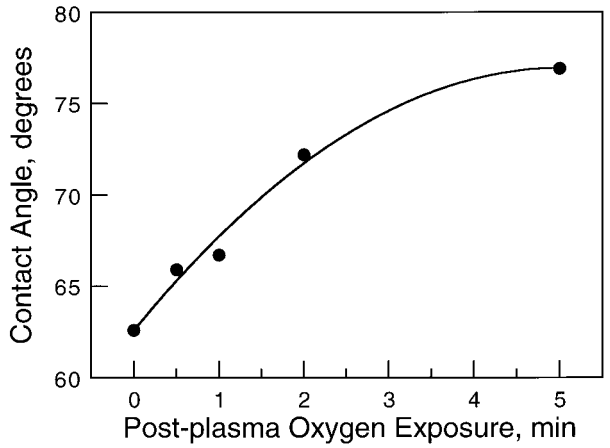

Figure 16 Contact angles of water on undrawn UHMWPE films exposed to oxygen after etching in Ar at 5 W.

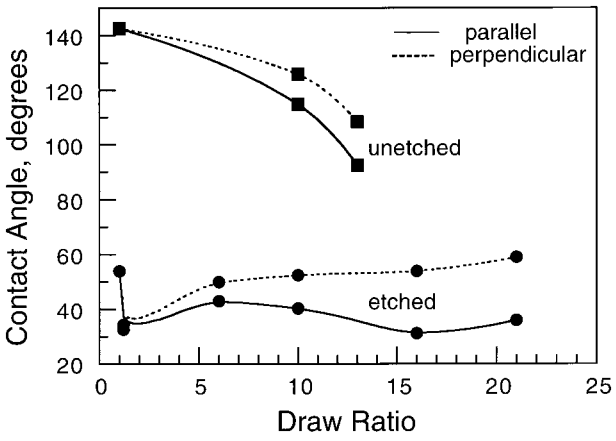

Figure 17 Contact angles of distilled water measured parallel and perpendicular to fibril orientation on UHMWPE films: (■) unetched, (●) etched, (——) parallel, and (- - -) perpendicular.

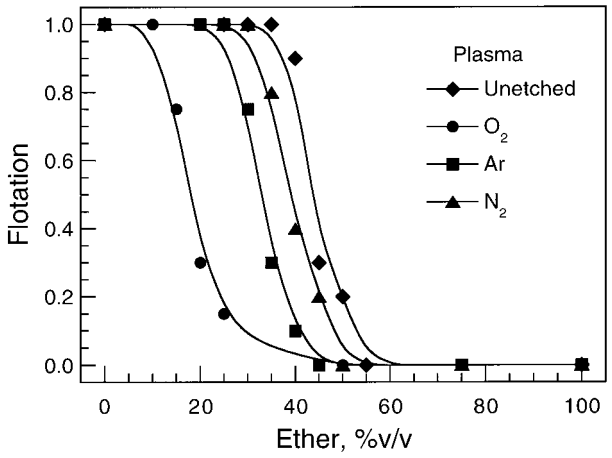

Figure 19 Flotation curves for UHMWPE fibers on benzylamine-ether solutions after plasma etching: (◆) unetched, (■) Ar, (▲) N_2, and (●) O_2.

equivalent to a reduction in contact angle and is consistent with previous work.[9] The fiber flotation technique also is sensitive enough to distinguish between the effects of the different plasmas (Fig. 19).

The as-received fibers are covered by a smooth low molecular weight weak boundary layer as seen in Figure 20(a).[9,26] The CA etching can remove this boundary layer and expose the fibrillar structure of the oriented UHMWPE. Etching with an argon plasma yields a slight increase in roughness [Fig. 20(b)] and a correspondingly slight enhancement in wetting (Fig. 19). Etching with a nitrogen plasma yields a larger increase in roughness, revealing the oriented fibrils [Fig. 20(c)], and a larger enhancement in wetting (Fig. 19). These results are similar to those obtained with CA etching.[9]

Etching with oxygen is a harsh treatment. Not only did the oxygen plasma remove the weak boundary layer but it seemed to melt and degrade the fiber to a great depth leaving a very rough surface containing deep flaws [Fig. 20(d)]. Although this harsh process yields a large enhancement in wetting (Fig. 19) it also causes a large reduction in mechanical properties.

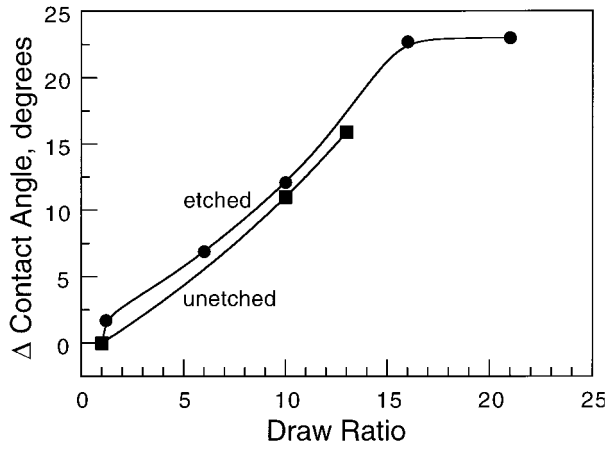

Figure 18 Differences in the contact angles measured parallel and perpendicular to fibril orientation from Figure 17 on UHMWPE films: (■) unetched and (●) etched.

CONCLUSIONS

Overall, the effects of surface modification on gel-cast and drawn UHMWPE films and gel-spun and drawn UHMWPE fibers are similar indicating that the films can be used as a model system for the fibers.

- A fibrillar hierarchical structure with significantly increased crystalline orientation and perfection is produced on drawing gel-cast UHMWPE films. These changes in structure increase modulus and strength by more than an order of magnitude. The effects of etching on the fibrillar structure, crystalline orientation, and mechanical properties of the drawn films are small compared with the effects of drawing.
- The reduction in upper melting point and degree of crystallinity on oxygen plasma

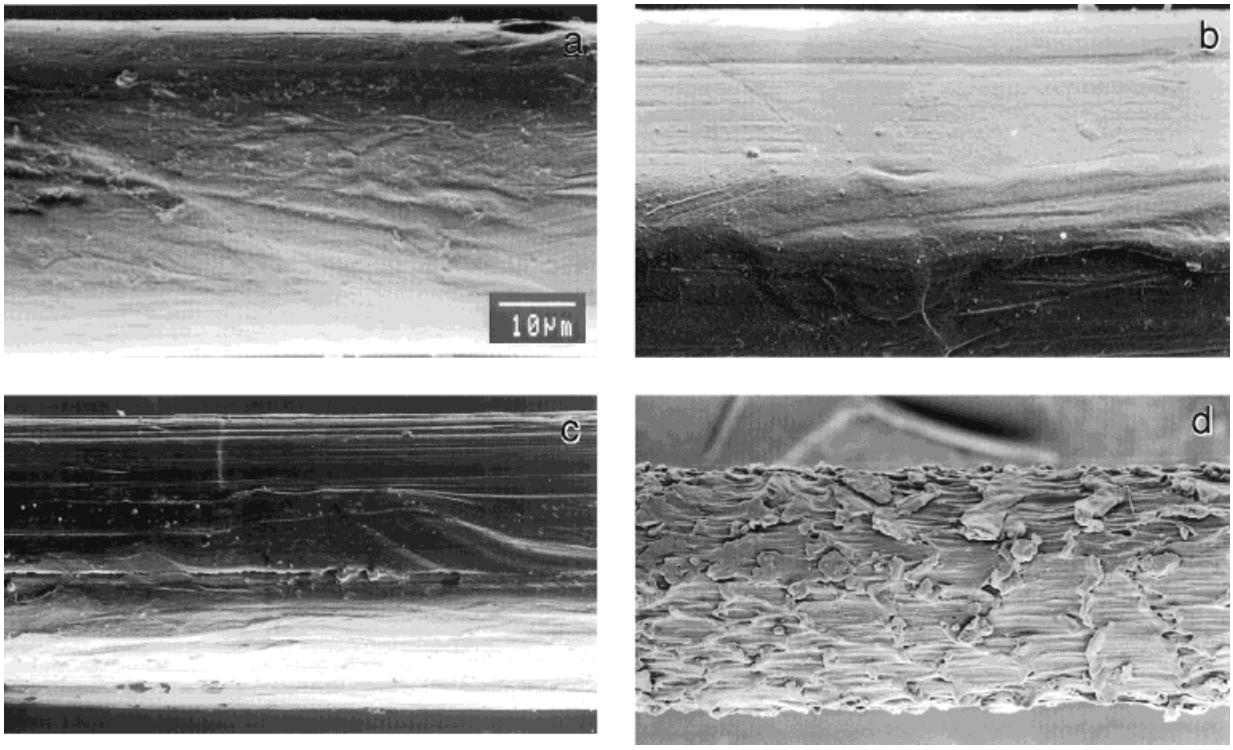

Figure 20 SEM micrographs of UHMWPE fibers after plasma etching: (a) unetched, (b) Ar, (c) N_2, and (d) O_2.

etching may result from changes in crystalline orientation and perfection caused by heating. The surface heating affects a larger proportion of the bulk for a thin film than for a molded section. The thickness decreases and melting point increases with drawing yielding an increase in heating and in melting point reduction.

- The relatively smooth, oxygen-free drawn films could not be bonded with epoxy whereas the rougher, more oxidized as-cast films formed a good bond. Etching roughened and oxidized the surface enhancing wetting and adhesion to epoxy for the undrawn and drawn films. The ILSS is highest for the etched drawn films because good adhesion yields a cohesive failure in the stronger drawn UHMWPE. Under the harsher oxygen plasma etching there is both cohesive failure in the UHMWPE and failure at the epoxy–UHMWPE interface.
- Nitrogen plasma etching at 100 W for 2 min was the optimum fiber etching process for increasing wetting among those studied. The nitrogen plasma both removed the low molecular weight layer on the surface, revealing the fibrillar topography, and etched the UHMWPE. Oxygen plasma etching was a harsh treatment that caused intensive degradation of the surface yielding enhanced wetting at the expense of a great reduction in mechanical properties.
- Contact angle measurements parallel to fibril orientation and fiber flotation on ether-benzylamine solutions were used successfully to study the wetting of fibrillar UHMWPE films and fibers, respectively.

The Technion V.P.R. Fund and the Fund for the Promotion of Research at the Technion provided partial support for this work.

REFERENCES

1. Barham, P. J.; Keller, A. J Mater Sci 1985, 20, 2281.
2. Capaccio, G.; Gibson, A. G.; Ward, I. M. in Ultra High Modulus Polymers; Ciferri, A., Ward, I. M., Eds.; Applied Science Publishers: London, 1979; p. 1.
3. Tissington, B.; Pollard, G.; Ward, I. M. J Mater Sci 1991, 26, 82.

4. Wu, S. Polymer Interface and Adhesion; Marcel Dekker: New York, 1982.
5. Kinloch, A. J. Adhesion and Adhesives; Chapman & Hall: New York, 1987.
6. Briggs, D.; Brewis, D. M.; Konieczo, M. B. J Mater Sci 1976, 11, 1270.
7. Briggs, D. in Surface Analysis and Pretreatment of Plastics and Metals; Brewis, D. M., Ed.; MacMillan: New York, 1982; p. 199.
8. Silverstein, M. S.; Breuer, O. J Mater Sci 1993, 28, 4153.
9. Silverstein, M. S.; Breuer, O. J Mater Sci 1993, 28, 4718.
10. Silverstein, M. S.; Breuer, O.; Dodiuk, H. J Appl Polym Sci 1994, 52, 1785.
11. Silverstein, M. S.; Breuer, O. Polymer 1993, 34, 3421.
12. Silverstein, M. S.; Breuer, O. Comp Sci Technol 1993, 12, 35.
13. Nardin, M.; Ward, I. M. Mater Sci Technol 1987, 3, 814.
14. Hild, D. N.; Schwartz, P. J Adhesion Sci Technol 1992, 6, 879.
15. Hild, D. N.; Schwartz, P. J Adhesion Sci Technol 1992, 6, 897.
16. Tissington, B.; Pollard, G.; Ward, I. M. Comp Sci Technol 1992, 44, 185.
17. Tissington, B.; Pollard, G.; Ward, I. M. J Mater Sci 1991, 26, 82.
18. Mercx, F. P. M. Polymer 1994, 35, 2098.
19. Inagaki, N.; Tadaka, S.; Kawai, H.; Kimura, Y. J Adhesion Sci Technol 1990, 4, 99.
20. Smith, P.; Lemstra, P. J.; Booij, H. C. J Polym Sci: Polym Phys 1981, 19, 877.
21. Smith, P.; Lemstra, P. J.; Pijpers, J. P. L.; Kiel, A. M. Colloid Polym Sci 1981, 259, 1070.
22. Lemstra, P. J.; Smith, P. Br Polym J 1980, 12, 212.
23. Smith, P.; Lemstra, P. J. Colloid Polym Sci 1980, 258, 891.
24. Sakai, Y.; Umetsu, K.; Miyasaka, K. Polymer 1993, 34, 318.
25. Krisyuk, B. E.; Marikhin, V. A.; Myasnikova, L. P.; Zaalishvili, N. L. Int J Polymeric Mater 1993, 22, 161.
26. Silverstein, M. S.; Sadovsky, J. J Adhesion Sci Technol 1995, 9, 1193.
27. Quirk, R. P.; Alsamarraie, M. A. A. in Polymer Handbook, 3rd Ed.; Brandrup, J., Immergut, E. H., Eds.; John Wiley: New York, 1989; p. V/15.
28. Jasper, J. J. J Phys Chem Ref Data 1972, 1, 841.
29. Adamson, A. W. A Textbook of Physical Chemistry, 3rd ed.; Academic Press: New York, 1986; p. 348.
30. Kaito, A.; Nakayama, K.; Kanetsuna, H. Polym J 1982, 14, 7571.
31. Smith, P.; Lemstra, P. J. J Mater Sci 1980, 15, 505.
32. Hoogstein, W.; ten Brinke, G.; Pennings, A. J. Colloid Polym Sci 1988, 266, 1003.
33. Penning, J. P.; Djikstra, D. J.; Pennings, A. J. J Mater Sci 1991, 26, 4721.
34. Anandakumaran, K.; Roy, S. K.; St. John Manley, R. Macromolecules 1988, 21, 1746.
35. Hummel, D. O. Atlas of Polymer and Plastics Analysis, Vol. 2; VCH Publishers: New York, 1988.
36. Garton, A. Infrared Spectroscopy of Polymer Blends, Composites and Surfaces; Hanser Publishers: Munich, 1992.
37. Ohta, T.; Wachi, T.; Nagai, T.; Takada, A.; Ikoda, Y.; Ohtsubo, T.; Kawaguchi, A. Polymer 1993, 34, 4863.